has a–d occupied, and the two Y_5 compounds have a–e occupied. To go beyond mere geometric description, and to understand the stability of these octahedral fragments, note that every triangular Y_3 face is capped by a monoanionic μ_3 ligand (Cl^- or OR^-). This makes the unifying feature of all observed structures the achievement of coordination number six for yttrium,[18] generally as a (distorted) octahedron. In this context, the (surprising!) incorporation of an oxo ligand is most efficient and compliant since it can be three-coordinate, four-coordinate or five-coordinate[19] and thus can serve to complete the favored coordination number of three, four, or even five yttrium centers.

The lack of a suitable cation under the conditions of eq 1 probably favors the formation of molecular (i.e., uncharged) reaction products; molecular reactants favor production of molecular (i.e., uncharged) reaction products. Thus, complete encapsulation of oxygen, to give $Y_6O(\mu_2\text{-}OR)_{12}(OR)_6^{2-}$, is perhaps not observed in eq 1 due in part to lack of a suitable partner cation.

The problem of achieving coordination number six in a molecular species is more readily accomplished for tetravalent metals (e.g., $U_3O(O^tBu)_{10}$,[20] $Zr_3S(S^tBu)_{10}$,[21] and $Mo_3O(OCH_2{}^tBu)_{10}$[22]) than for trivalent metals, since fewer anionic ligands are available in the latter case. One solution to this problem for trivalent metals is to aggregate more than three metals into a closed polyhedral fragment. In this way, the ratio of bridging to terminal ligands increases, thereby increasing the coordination number of each metal. The tolerance of O^{2-} to bind simultaneously a large number of metals also favors its incorporation.

The hypothesis that it is the yttrium coordination number that dictates product stoichiometry (identity) quite naturally explains the retention of two THF molecules in two isomers of $Y_3Cl(O^tBu)_8(THF)_2$ and in $La_3(O^tBu)_9(THF)_2$. This hypothesis predicts that a tetrahedron is an unsuitable polyhedron for a $Y_4(\mu_4\text{-}O)$ cluster since $(YOR)_4O(\mu_2\text{-}OR)_6$ has only five-coordinate yttrium. It likewise rationalizes why the reported Y_4O species is a "butterfly" and not planar (inefficient use of oxide ligand and its orbitals) as well as why it retains two chloride ligands: hypothetical $(YO^tBu)_4O(\mu_2\text{-}O^tBu)_4(\mu_3\text{-}O^tBu)_2$ would have two five-coordinate metal centers (at the "wingtips"), each of which is observed to bind one chloride.

A final question revolves around why the synthesis reported here does not yield a stable $Y_3O(O^iPr)_7(^iPrOH)_3$, structural unit similar to that of $Y_3Cl(O^tBu)_8(THF)_2$. We suggest that this is a combination of the more appropriate size and greater donor character of O vs Cl, and the smaller size of O^iPr with respect to O^tBu. The occurrence of a $Y_5O(OR)_8$ core both in this synthesis and from the reaction of KOMe-MeOH with $(\eta^5\text{-}Cp)_2YCl(THF)$[12] suggests special stability for this structural unit. The solubility of $Y_5O(OR)_{13}$, as well as the lability of the alkoxide ligands, allows its use as molecular precursors for multicomponent yttrium oxide materials by hydrolysis.[23]

Acknowledgment. Support by the CNRS (AIR and GRECO 93 "Précurseurs Moléculaires de Matériaux Inorganiques"), by Rhône-Poulenc (to L.G.H.-P.), and by the U.S. National Science Foundation and Union Molycorp (to K.G.C.) is acknowledged. W.J.S. was a Chester Davis Postdoctoral Fellow during part of this project. We are also grateful to Dr. M. Bourdonneau (Laboratoire d'Applications Bruker France) for obtaining the ^{89}Y NMR spectra.

Supplementary Material Available: Anisotropic thermal parameters (Table SI) and complete bond lengths and angles (Table SII) (7 pages); tables of observed and calculated structure factors (4 pages). Ordering information is given on any current masthead page.

(18) Yttrium is also six-coordinate in Y_2O_3. See: O'Connor, B. H.; Valentine, T. M. *Acta Crystallogr.* **1969**, *B25*, 2140.
(19) Bottomley, F.; Sutin, L. *Adv. Organomet. Chem.* **1988**, *28*, 339.
(20) Cotton, F. A.; Marler, D. O.; Schwotzer, W. *Inorg. Chim. Acta* **1984**, *95*, 207.
(21) Coucouvanis, D.; Hadjikyriacou, A.; Kanatzidis, M. G. *J. Chem. Soc., Chem. Commun.* **1985**, 1224.
(22) Chisholm, M. H.; Folting, K.; Huffman, J. C.; Kirkpatrick, C. C. *Inorg. Chem.* **1984**, *23*, 1021.
(23) Chaput, F.; Boilot, J. P.; El Khokh, N.; Papiernik, R.; Hubert-Pfalzgraf, L. G. Presented at the French Chemical Society Meeting, Nice, Sept 1988.

Contribution from the Department of Chemistry, North Carolina State University, Raleigh, North Carolina 27695-8204, Laboratoire de Chimie Théorique, Bât. 490, Université de Paris-Sud, 91405 Orsay, France, and Institute de Physique et Chimie des Materiaux (UA CNRS 279), Université de Nantes, 44072 Nantes, France

Structural Origin of Semiconducting Properties of the Molybdenum Red Bronzes $A_{0.33}MoO_3$ (A = K, Rb, Cs, Tl)

Myung-Hwan Whangbo,*[†] Michel Evain,[†] Enric Canadell,*[‡] and Marcel Ganne[§]

Received September 29, 1988

Tight-binding band structure calculations were performed on the molybdenum red bronzes $Cs_{0.33}MoO_3$ and $Tl_{0.33}MoO_3$ to examine whether they are regular semiconductors or Mott insulators. Our calculations show that these red bronzes have a band gap and that their valence and conduction bands are as wide as those calculated for the blue bronze $K_{0.3}MoO_3$, which is a metal at room temperature. Thus, the red bronzes $A_{0.33}MoO_3$ (A = K, Rb, Cs, Tl) are not Mott insulators but regular semiconductors. Our analysis of the t_{2g}-block band orbitals reveals that the band gap of the red bronzes occurs as a direct consequence of the O–Mo···O alternations in their MoO_6 octahedra.

Molybdenum bronzes refer to a class of solid oxide phases of composition $A_xMo_yO_z$, where A is an alkali metal or Tl, and exhibit intense color and metallic luster. Recently, physical properties of several molybdenum bronzes have extensively been studied in connection with the charge density wave phenomenon arising from their low-dimensional metallic character.[1-3] In the molybdenum bronze, alkali metal or Tl donates its valence electron to the transition metal, so that the nature of its low-lying d-block bands determines whether the bronze is a metal or a semiconductor. Alkali-metal molybdenum oxides are classified into three

[†] North Carolina State University.
[‡] Université de Paris-Sud.
[§] Université de Nantes.

(1) (a) Schlenker, C.; Dumas, J. *Crystal Structures and Properties of Materials with Quasi One-Dimensional Structures*; Rouxel, J., Ed.; Reidel: Dordrecht, The Netherlands, 1986; p 135. (b) Greenblatt, M. *Chem. Rev.* **1988**, *88*, 31.
(2) (a) Wold, A.; Kunnmann, W.; Arnott, R. J.; Ferretti, A. *Inorg. Chem.* **1964**, *3*, 345. (b) Stephenson, N. C.; Wadsley, A. D. *Acta Crystallogr.* **1965**, *18*, 241. (c) Bouchard, G. H.; Perlstein, J. H.; Sienko, M. J. *Inorg. Chem.* **1967**, *6*, 1682. (d) Pouget, J. P.; Noguera, C.; Moudden, A. H.; Moret, T. *J. Phys. (Les Ulis, Fr.)* **1985**, *46*, 1731. (e) Pouget, J. P.; Kagoshima, S.; Schlenker, C.; Marcus, J. *J. Phys. Lett.* **1983**, *44*, L113. (f) Fleming, R. M.; Schneemeyer, L. F.; Moncton, D. E. *Phys. Rev. B: Condens. Matter* **1985**, *31*, 899. (g) Sato, M.; Fujishita, H.; Hoshino, S. *J. Phys. C* **1985**, *18*, 2603.

0020-1669/89/1328-0267$01.50/0

groups:[1] blue bronzes $A_{0.3}MoO_3$,[1,2] purple bronzes $A_{0.9}Mo_6O_{17}$,[1,3] and red bronzes $A_{0.33}MoO_3$.[1,4] The blue and purple bronzes are metals at room temperature but exhibit resistivity anomalies at low temperature.[1,3] These electrical properties of the blue and purple bronzes have recently been explained on the basis of their band electronic structures.[5]

All red bronzes $A_{0.33}MoO_3$ (A = Li, K, Rb, Cs, Tl) are found to be semiconductors.[4a-c] $Li_{0.33}MoO_3$[4d] has a three-dimensional structure in that it contains neither isolated metal–oxygen chains nor isolated metal–oxygen layers. A band electronic structure study[6] suggests that this red bronze is a regular semiconductor. Other red bronzes $A_{0.33}MoO_3$ (A = K, Rb, Cs, Tl)[4b,d-f] consist of isolated layers of composition MoO_3, and hence may be referred to as two-dimensional (2D) red bronzes. The Mo–O bonds of the 2D red bronze $K_{0.33}MoO_3$ are slightly longer than those of the blue bronze $K_{0.3}MoO_3$. On the basis of this observation, Travaglini and Wachter proposed[7] that the 2D red bronze $K_{0.33}MoO_3$ is not a regular semiconductor (i.e., one that has no partially filled bands in a one-electron band picture) but a Mott insulator[8] (i.e., a semiconductor or an insulator despite the presence of partially filled bands in a one-electron band picture). The insulating property of Mott insulators originates from electron localization, which is caused by electron–electron repulsion.[8] In general, a system with a partially filled band is expected to be a Mott insulator when its bandwidth, W, is narrow (precisely speaking, when W is smaller than the on-site repulsion, U).[8] The d-block bandwidths of molybdenum bronzes increase with the overlap between molybdenum d orbitals and bridging-oxygen p orbitals. Therefore, it is not surprising to speculate[7] that the longer Mo–O bonds of the 2D red bronze $K_{0.33}MoO_3$ (with respect to those of the blue bronze $K_{0.3}MoO_3$) might provide a narrow enough band susceptible to Mott electron localization.

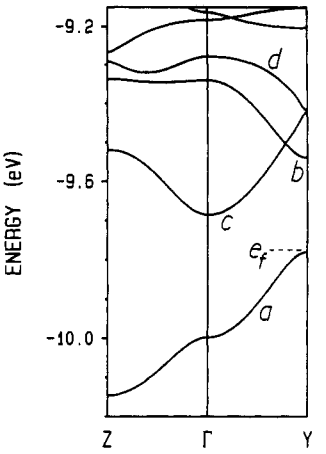

Figure 1. Bottom portion of the t_{2g}-block bands of the real Mo_6O_{18} layer. In units of the reciprocal vectors a^*, b^*, and c^*, the points Γ, Y, and Z are defined as Γ = (0, 0, 0), Y = (0, $b^*/2$, 0), and Z = (0, 0, $c^*/2$).

However, magnetic susceptibility and ESR studies[4b,9] suggest that the 2D red bronzes have delocalized d electrons and have very little spin density. These findings are not consistent with the proposal that the 2D red bronzes are Mott insulators. To examine whether the 2D red bronzes are regular semiconductors or Mott insulators, we performed tight-binding band structure calculations[10] on $Cs_{0.33}MoO_3$ and $Tl_{0.33}MoO_3$ within the framework of the extended Hückel method.[11] The atomic parameters used in this work are identical with those employed for our earlier work on the blue bronze $K_{0.33}MoO_3$[5a] and the purple bronzes $K_{0.9}Mo_6O_{17}$[5b] and $Li_{0.9}Mo_6O_{17}$.[5c] The band electronic structures calculated for $Tl_{0.33}MoO_3$ and $Cs_{0.33}MoO_3$ are practically identical, and thus we discuss only those results concerning $Tl_{0.33}MoO_3$ in the following sections.

Crystal Structure

In analyzing how the band electronic structures of the 2D bronzes are related to their crystal structures, it is convenient to construct the crystal structures in terms of the Mo_6O_{26} clusters **1**.[6] Upon sharing the corners of the Mo_6O_{26} clusters, one obtains

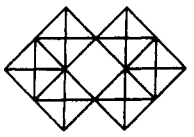

1

the Mo_6O_{24} chain **2**. Removal of the hump MoO_6 octahedra (i.e.,

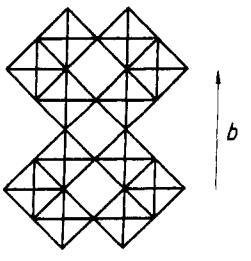

2

(3) (a) Vincent, H.; Ghedira, M.; Marcus, J.; Mercier, J.; Schlenker, C. *J. Solid State Chem.* **1983**, *47*, 113. (b) Buder, R.; Devenyi, J.; Dumas, J.; Marcus, J.; Mercier, J.; Schlenker, C. *J. Phys. (Les Ulis, Fr.)* **1982**, *43*, L59. (c) Bervas, E.; Cochrane, R. W.; Dumas, J.; Escribe-Filippini, C.; Marcus, J.; Schlenker, C. *Lect. Notes Phys.* **1985**, *217*, 144. (d) Dumas, J.; Bervas, E.; Marcus, J.; Salomon, D.; Schlenker, C. *J. Magn. Magn. Mater.* **1983**, *31–34*, 535. (e) Escribe-Filippini, C.; Konate, K.; Marcus, J.; Schlenker, C.; Almairac, R.; Ayrolles, R.; Roucau, C. *Philos. Mag. B* **1984**, *50*, 321. (f) Gatehouse, B. M.; Lloyd, D. J.; Miskin, B. K. *NBS Spec. Publ. (U.S.)* **1972**, *No. 364*, 15. (g) Stephenson, N. C. *Acta Crystallogr.* **1966**, *20*, 59. (h) Greenblatt, M.; Ramanujachary, K. V.; McCarroll, W. H.; Neifeld, R.; Waszczak, J. V. *J. Solid State Chem.* **1985**, *59*, 149. (i) Ganne, M.; Dion, M.; Boumaza, A.; Tournoux, M. *Solid State Commun.* **1986**, *59*, 137. (j) Ramanujachari, K. V.; Collins, B. T.; Greenblatt, M. *Solid State Commun.* **1986**, *59*, 647. (k) Onoda, M.; Toriumi, K.; Matsuda, Y.; Sato, M. J. *Solid State Chem.* **1987**, *66*, 163. (l) Schlenker, C.; Schwenk, H.; Escribe-Filippini, C.; Marcus, J. *Physica B+C* **1985**, *135B*, 511. (m) Greenblatt, M.; McCarroll, W. H.; Neifeld, R.; Croft, M.; Waszcczak, J. V. *Solid State Commun.* **1984**, *51*, 671. (n) Ramanujachari, K. V.; Collins, B. T.; Greenblatt, M.; McNally, P.; McCarroll, W. H. *Solid State Ionics* **1986**, *22*, 105. (o) Matsuda, Y.; Onoda, M.; Sato, M. *Physica B+C* **1986**, *143B+C*, 243.

(4) (a) Travaglini, G.; Wachter, P.; Marcus, J.; Schlenker, C. *Solid State Commun.* **1982**, *42*, 407. (b) Ganne, M.; Dion, M.; Boumaza, A. *C. R. Acad. Sci., Ser. 2* **1986**, *302*, 635. (c) Strobel, P.; Greenblatt, M. *J. Solid State Chem.* **1981**, *36*, 331. (d) Tsai, P. P.; Potenza, J. A.; Greenblatt, M. *J. Solid State Chem.* **1987**, *69*, 329. (e) Stephenson, N. C.; Wadsley, A. D. *Acta Crystallogr.* **1965**, *18*, 241. (f) Rêau, J.-M.; Fouassier, C.; Hagenmuller, P. *Bull. Soc. Chim. Fr.* **1971**, *8*, 2884. (g) Morsli, M.; Bonnet, A.; Connan, A.; Ganne, M.; Jouanneaux *Phys. Rev. B.: Condens. Matter*, in press.

(5) (a) Whangbo, M.-H.; Schneemeyer, L. F. *Inorg. Chem.* **1986**, *25*, 2424. (b) Whangbo, M.-H.; Canadell, E.; Schlenker, C. *J. Am. Chem. Soc.* **1987**, *109*, 6308. (c) Whangbo, M.-H.; Canadell, E. *J. Am. Chem. Soc.* **1988**, *110*, 358.

(6) Canadell, E.; Whangbo, M.-H. *Inorg. Chem.* **1988**, *27*, 228.

(7) Travaglini, G.; Wachter, P. *Solid State Commun.* **1983**, *47*, 217.

(8) (a) Mott, N. F. *Metal-Insulator Transitions*; Barnes and Noble: New York, 1977. (b) Brandow, B. H. *Adv. Phys.* **1977**, *26*, 651. (c) Whangbo, M.-H. *Acc. Chem. Res.* **1983**, *16*, 95; *J. Chem. Phys.* **1979**, *70*, 4963.

(9) Bang, G.; Sperlich, G. *Z. Phys. B* **1975**, *22*, 1.

(10) Whangbo, M.-H.; Hoffmann, R. *J. Am. Chem. Soc.* **1978**, *100*, 6093.

(11) Hoffmann, R. *J. Chem. Phys.* **1963**, *39*, 1399. A modified Wolfsberg–Helmholz formula was used to calculate the off-diagonal H_{ij} values: Ammeter, J. H.; Bürgi, H.-B.; Thibeault, J.; Hoffmann, R. *J. Am. Chem. Soc.* **1978**, *100*, 3686.

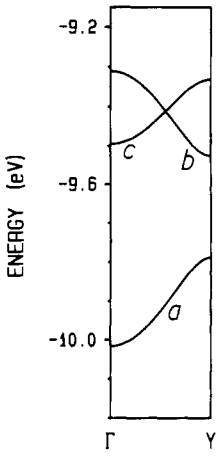

Figure 2. Bottom portion of the t_{2g}-block bands of the real Mo_4O_{18} chain.

those that do not form a continuous chain) from **2** leads to the Mo_4O_{18} chain **3**.

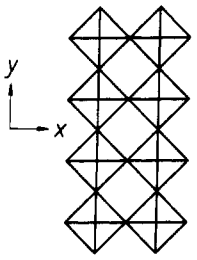

3

A projection view of **2** along the chain direction can be represented by **4**. Then the Mo_6O_{18} layer (i.e., MoO_3 layer) **5** is

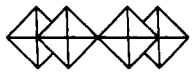

4

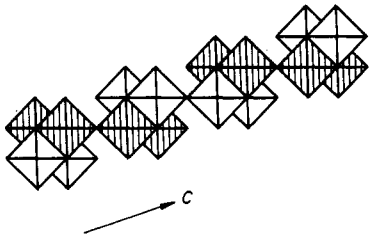

5

obtained by sharing the corners and edges of the Mo_6O_{24} chains. For the purpose of clarity, every second Mo_6O_{24} chain is shaded in **5**. In the 2D red bronzes $A_{0.33}MoO_3$, the Mo_6O_{18} layers **5** alternate with the layers of the cations A^+ along the crystallographic *a* direction. If the hump octahedra are removed from **5**, one obtains the Mo_4O_{14} layer **6**.

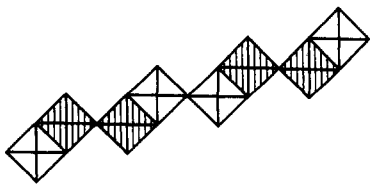

6

Band Electronic Structure

Figure 1 shows the dispersion relations for the bottom portion of the t_{2g}-block bands of $Tl_{0.33}MoO_3$. With two electrons to fill these bands (i.e., $^1/_3$ for MoO_3 or 2 for Mo_6O_{18}), only the bottom band a is filled so that an indirect band gap of about 0.12 eV exists between bands a and c. Furthermore, these bands are as dispersive as the corresponding bands calculated for the blue bronze $K_{0.3}MoO_3$.[5a] Thus, the 2D red bronzes cannot be Mott insulators, which are characterized by partially filled narrow bands.[8] According to the present study, therefore, the 2D red bronzes are not Mott insulators but regular semiconductors.

Our result that the lowest lying t_{2g}-block band is separated from those bands lying above with an indirect band gap of ~0.12 eV is consistent with several experimental observations: the optical reflectivity of the red bronze $K_{0.33}MoO_3$ suggests a band gap of 0.5 eV,[4a] and the temperature dependence of the resistivity in $Cs_{0.33}MoO_3$[4c] and $Tl_{0.33}MoO_3$[4b,g] indicates a band gap of 0.24 and 0.52 eV, respectively.

For the purpose of comparison, Figure 2 shows the dispersion relations for the bottom portion of the t_{2g}-block bands of the Mo_4O_{18} chain **3**. Those bands are very similar in nature to the corresponding ones of the Mo_6O_{18} layer (in the $\Gamma \rightarrow Y$ region), except for the minor difference that band c is slightly lower in energy in the Mo_6O_{18} layer than in the Mo_4O_{18} chain. Thus, in understanding why an energy gap exists between bands a and c of the Mo_6O_{18} layer (and hence in the red bronze), it is necessary to analyze why the corresponding band gap occurs in the Mo_4O_{18} chain. This is discussed in the following section.

Band Gap and O–Mo···O Alternation

A. t_{2g}-Level Splitting. The nature of the t_{2g}-block bands of $Li_{0.33}MoO_3$ critically depends upon the Mo–O bond length variation.[6] For a regular MoO_6 octahedron **7a**, the t_{2g}-block levels

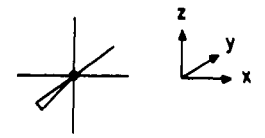

7a

7b

may be represented by **7b**. Though omitted for simplicity in **7b**, the oxygen orbitals combine out-of-phase with the metal orbitals. Thus, in general, the t_{2g}-block levels are raised when the Mo–O bond is shortened. The Mo–O bond shortening **7a** → **8a** leads

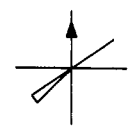

8a

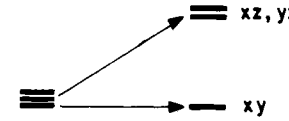

8b

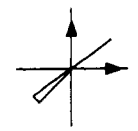

9a

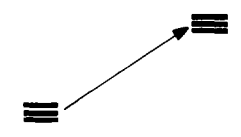

9b

to the t_{2g}-level splitting shown in **8b**. That is, the **7a** → **8a** distortion raises the π orbitals but leaves the δ orbital intact. (Here, the π and δ symmetry elements are taken with respect to the shortened Mo–O bond axis.) When the Mo atom of **7a** moves along the diagonal direction between two orthogonal Mo–O bonds as described in **9a**, all the t_{2g} levels are raised in energy as shown in **9b**. Thus, in a system that has both the **7a** → **8a** and the **7a**

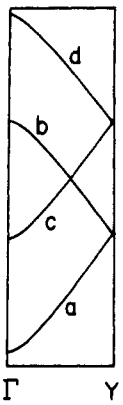

Figure 3. *xy* bands of the ideal Mo_4O_{18} chain.

→ **9a** distortions, the bottom t_{2g}-block level of **8b** will become the lowest lying d-block level.

Shown in **10** and **11** are the various Mo–O bond lengths found in the Mo_6O_{18} layers of $Tl_{0.33}MoO_3$. The hump octahedra have

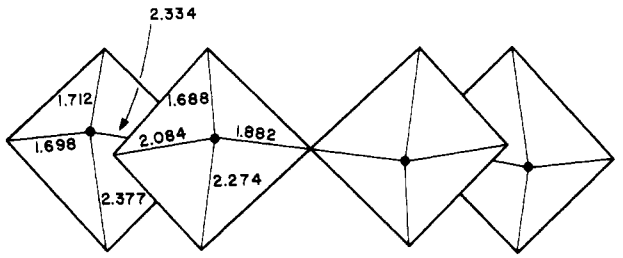

10

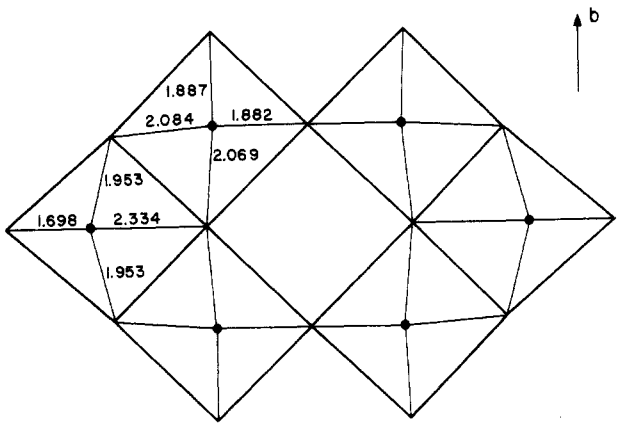

11

a strong O–Mo···O bond alternation of type **7a** → **9a**, while the chain octahedra (i.e., those that are a part of the Mo_4O_{18} chain) have a strong O–Mo···O alternation of type **7a** → **8a** along the direction perpendicular to the chain axis. Thus, the t_{2g}-block levels of the hump octahedra are high in energy. Among the t_{2g}-block levels of each chain octahedron, only one d level that is a δ orbital with respect to the shortened Mo–O bond (perpendicular to the chain axis) remains low in energy. This orbital, which may be chosen as an *xy* orbital without loss of generality, makes a π-type overlap with the oxygen p orbital along the chain axis (vide infra). Thus, it is sufficient to consider only the *xy* bands of the Mo_4O_{18} chain in describing the nature of the low-lying d-block bands of the Mo_6O_{18} layer.

B. *xy* Bands of the Mo_4O_{18} Chain. Figure 3 shows the *xy* bands of the ideal Mo_4O_{18} chain in which all MoO_6 octahedra are regular.[5] Shown in **12** are cluster orbitals relevant for band orbital construction. It is obvious from **12** that the energies of these orbitals increase in the order **12a** < **12b**, **12c** < **12d**. Band a at Γ has the nodal property **13**. Bands a and b at *Y* have the nodal

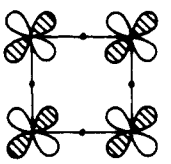

12a

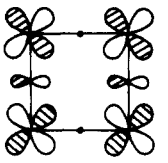

12b

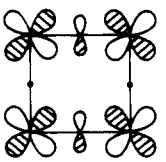

12c

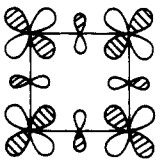

12d

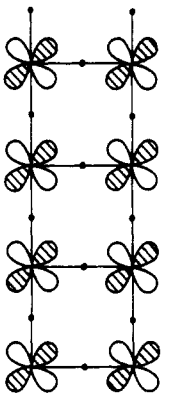

13

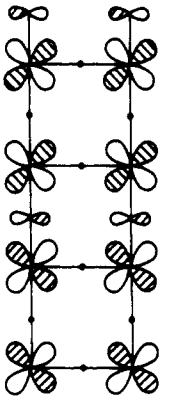

14

properties **14** and **15**, respectively. Band c at Γ has the nodal

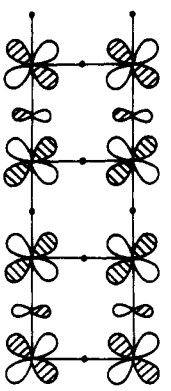

15

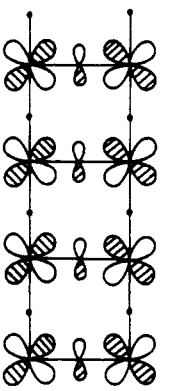

16

property **16**. For the ideal Mo_4O_{18} chain, bands a and b at *Y* are degenerate with band c at Γ. Eventually, how this degeneracy is lifted in the real Mo_4O_{18} chain determines the band gap of the real Mo_6O_{18} layer.

As can be seen from **11**, there exists a bond length alternation of the type Mo···O···Mo–O–Mo along the chain (i.e., 2.069, 2.069, 1.887, and 1.887 Å). This destroys the degeneracy between **14** and **15**. The short Mo–O bonds (1.882 Å) in the Mo–O–Mo linkages of **10**, perpendicular to the chain, are comparable to the short Mo–O bonds (1.887 Å) of **11** along the chain. Thus, in the real Mo_4O_{18} chain, the extents of Mo–O antibonding in **15** and **16** are comparable. Therefore, band a at *Y* is lowered, while band b at *Y* and band c at Γ are raised in energy when the Mo_4O_{18} chain distorts from the ideal to the real structure. This is why the real Mo_4O_{18} chain has a band gap.

C. Interchain Interactions via Hump Octahedra. We now examine how the t_{2g}-block bands of the real Mo_4O_{18} chain are shifted in energy by the interchain interactions in the Mo_6O_{18} layer. Comparison of Figures 1 and 2 shows that band a remains unchanged in energy along Γ → *Y* but is lowered in energy along

$\Gamma \rightarrow Z$. Band c is shifted downward in energy along $\Gamma \rightarrow Y$ but is raised in energy along $\Gamma \rightarrow Z$.

When viewed along the chain, band orbitals **13**–**15** are represented by **17**, and band orbital **16** by **18**. With such representations, bands a and b of Figure 1 at Γ are described by **19**,

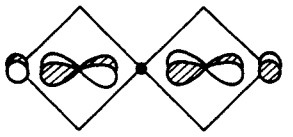

17

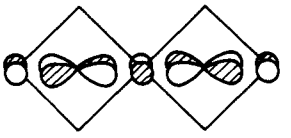

18

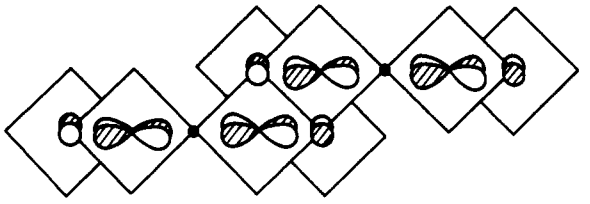

19

and band c of Figure 1 at Γ is described by **20**. Note from **19**

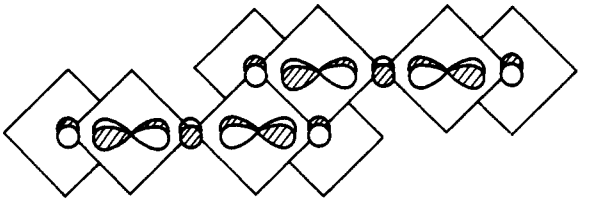

20

and **20** that the p orbital of each external oxygen atom of one Mo_4O_{18} chain is located along the nodal plane of the *xy* orbital of the adjacent Mo_4O_{18} chain. Thus, no direct interchain interactions are expected in the Mo_6O_{18} layer.

The essential orbital patterns of **19** and **20** around the hump MoO_6 octahedra are given by **21** and **22**, respectively. Since the

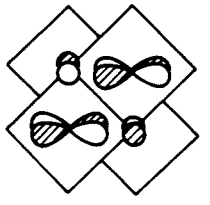

21

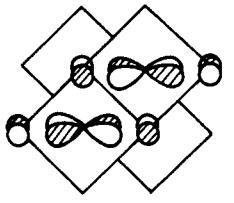

22

d-block levels of the hump octahedra are higher lying in energy, they act as acceptor orbitals; i.e., they combine in-phase with the chain d-block levels if allowed by symmetry. As illustrated in **23**

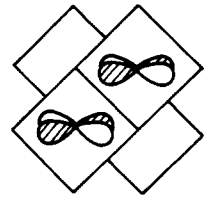

23

and **24**, the symmetry of **21** does not allow such a mixing but that

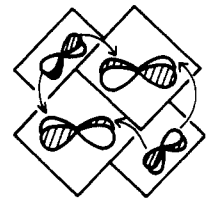

24

of **22** does. When this mixing occurs, the oxygen p-orbital contribution of the inner two oxygen atoms of **22** decreases because the p orbital is located close to the nodal plane of the *xy* orbital of the hump octahedron as shown in **25**. Along $\Gamma \rightarrow Y$, bands

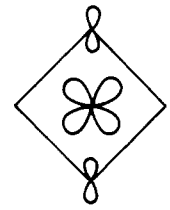

25

a and c retain the orbital characters **21** and **22**, respectively. Thus, the whole band c of the Mo_6O_{18} layer is lowered with respect to that of the Mo_4O_{18} chain, while band a remains unshifted. However, along $\Gamma \rightarrow Z$, the relative orbital phases between adjacent chains must change from in-phase to out-of-phase or vice versa. Therefore, bands a and c gradually pick up the orbital patterns of **22** and **21**, respectively. Therefore, along $\Gamma \rightarrow Z$, band a is lowered but band c is raised in energy.

Concluding Remarks

The present band structure calculations reveal that the 2D red bronzes $A_{0.33}MoO_3$ have a band gap and that their valence and conduction bands are as wide as those calculated for the blue bronze $A_{0.3}MoO_3$. Therefore, Mott localization is not responsible for the semiconducting properties of the 2D red bronzes. They are simply regular semiconductors. Our analysis of the t_{2g}-block band orbitals shows that the 2D red bronzes have a band gap as a direct consequence of the O–Mo···O bond alternation in their MoO_6 octahedra.

Acknowledgment. This work was supported by NATO, Scientific Affairs Division, and also by DOE, Office of Basic Sciences, Division of Materials Science, under Grant DE-FG05-86ER45259.